CRYSTAL GROWTH & DESIGN
2009
VOL. 9, NO. 1
182–191

Adaptive Concentration Control of Cooling and Antisolvent Crystallization with Laser Backscattering Measurement

Xing Yi Woo,[†,§] Zoltan K. Nagy,[‡] Reginald B. H. Tan,[§,||] and Richard D. Braatz*,[†]

University of Illinois at Urbana−Champaign, Urbana, Illinois 61801, Chemical Engineering Department, Loughborough University, Loughborough, LE11 3TU, United Kingdom, Department of Chemical and Biomolecular Engineering, National University of Singapore, 119260, Singapore, and Institute of Chemical and Engineering Sciences, 1 Pesek Road, Jurong Island, Singapore 627833

Received February 3, 2008; Revised Manuscript Received August 11, 2008

ABSTRACT: This paper presents a thorough simulation and experimental evaluation of the concentration control approach for batch and semibatch crystallization. The sensitivity of concentration feedback control is assessed in the case of various disturbances that result in excessive nucleation events. The enhanced robustness of the concentration control is demonstrated against the widely used direct operation approach, which directly implements the temperature or antisolvent addition rate versus time. An adaptive concentration control strategy is proposed that employs measurement of the number of particle counts per unit time provided by in situ laser backscattering, to detect the onset of nucleation and adapt the operating curve accordingly, further enhancing the robustness of the approach. Simulation and experimental results indicate that adaptive concentration control is robust to variations in the nucleation, growth, or dissolution rates due to scale-up or other changes in the process conditions.

1. Introduction

The control of industrial crystallization processes has received increased research attention in recent years.[1−3] This is motivated by the critical need to consistently meet the specifications on purity, crystal size and shape distributions, and polymorphic form in the crystallization of pharmaceuticals,[4] as well as the advancement of simulation and sensor technologies.[5,6] Along with the U.S. Food and Drug Administration's (FDA) initiative to introduce process analytical technologies (PAT) in the pharmaceutical industries, the development of control strategies to improve the performance of the manufacturing process, as well as the quality of the product, becomes increasingly important.[6−8]

One method for operating a pharmaceutical crystallization process is to follow a predetermined temperature or antisolvent composition (or addition rate) profile. A first-principles approach to the determination of the optimal profile, as well as seed characteristics and loading, involves solving an optimization defined by a performance objective and the process constraints.[9−14] A requirement of this approach is the need to simulate the crystallization process with accurate nucleation and growth kinetics determined in a series of experiments.[12,15−17] An important practical consideration is that the kinetic and thermodynamic parameters can vary substantially from batch to batch due to varying amounts of impurities. Optimal profiles computed for nominal parameters for crystallization processes can be very sensitive to these parameter variations as well as other disturbances.[18]

An alternative approach that does not require accurate kinetics or extensive experimentation is to adjust the cooling or antisolvent addition rate to follow a concentration (or supersaturation) profile within the metastable zone using feedback control based on in-process concentration measurement (see Figures 1 and 2).[19−21] This approach has been implemented successfully in the pharmaceutical industry and is commonly known as concentration control, supersaturation control, or direct design.[22−24] The main advantage of this approach is its insensitivity to most parameter variations and process disturbances. Recent applications demonstrate the advantages of using laser backscattering measurement in the feedback control of crystallization systems.[25−27]

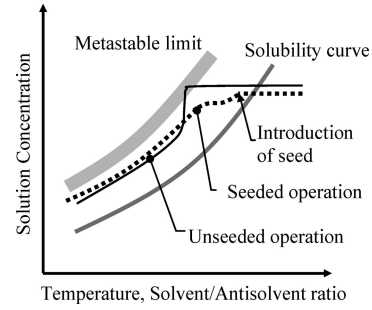

Figure 1. Phase diagram for seeded and unseeded batch cooling and antisolvent crystallization. Shown are the metastable zone, which is bounded by the solubility curve and metastable limit, and concentration−temperature or concentration−solvent/antisolvent ratio setpoint trajectories.

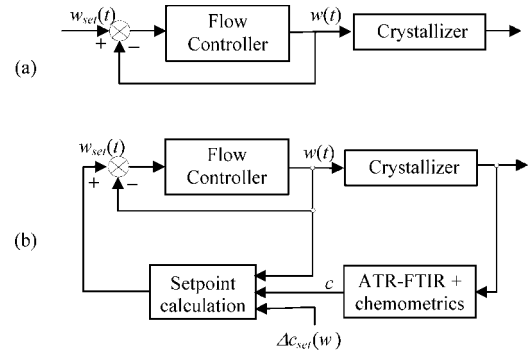

Figure 2. Schematic block diagrams for (a) antisolvent composition (w) versus time (t) approach and (b) concentration (c) versus w approach.

* Corresponding author. E-mail: braatz@uiuc.edu.
† University of Illinois at Urbana−Champaign.
§ National University of Singapore.
‡ Loughborough University.
|| Institute of Chemical and Engineering Sciences.

10.1021/cg800131r CCC: $40.75
Published on Web 11/20/2008

This paper provides a sensitivity and disturbance analysis of various control strategies with and without inclusion of laser backscattering measurement to increase robustness with respect to disturbances that result in excessive nucleation events. The first part of the paper provides an extensive evaluation of the sensitivities of concentration control in antisolvent crystallization for a wide range of process disturbances, which extends past work on cooling crystallization.[2,28] In the second part of the paper, experimental results with a novel adaptive concentration control approach are reported, which uses laser backscattering measurements to adapt, according to a dynamic feedback control algorithm, the operating curve within the metastable zone during the batch crystallization.

2. Concentration Control

Concentration control in crystallization processes involves the feedback control of temperature or antisolvent flow rate to maintain a preset supersaturation profile based on concentration measurements. The equations below consider the case of following a concentration setpoint based on constant supersaturation setpoint profile within the metastable limit for an antisolvent crystallizer (the cooling case is similar). The solute concentration at time k is

$$c_k = \frac{m_{\text{solute},k}}{m_{\text{solvent}} + m_{\text{antisolvent},k}} \tag{1}$$

and the setpoint concentration at the new time step, $k + 1$, is

$$c_{\text{setpoint}} = c_{k+1} = c^*(w_{k+1}) + \Delta c \tag{2}$$

where m is mass, w is antisolvent mass percent on a solute-free basis, and c^* is the saturated solution concentration as a function of w. Taking into account the dilution effect,

$$w_{k+1} = 100\left(\frac{m_{\text{antisolvent},k} + t_s\dot{m}_{\text{antisolvent},k+1}}{m_{\text{solvent}} + m_{\text{antisolvent},k} + t_s\dot{m}_{\text{antisolvent},k+1}}\right) \tag{3}$$

where $\dot{m}$ is the mass flow rate, and t_s is the sampling time. Since $m_{\text{solute},k+1} \approx m_{\text{solute},k}$ to very high accuracy when the sampling time is small,

$$c_{\text{setpoint}} = c_{k+1} = \frac{m_{\text{solute},k}}{m_{\text{solvent}} + m_{\text{antisolvent},k} + t_s\dot{m}_{\text{antisolvent},k+1}} \tag{4}$$

Combining the above equations gives the following equation to be solved to obtain w_{k+1}

$$c^*(w_{k+1}) + \Delta c + \frac{m_{\text{solute},k}}{m_{\text{solvent}}}\left(\frac{w_{k+1}}{100} - 1\right) = 0 \tag{5}$$

with $\dot{m}_{\text{antisolvent}}$ subsequently determined from eq 3. Equation 5 can also be applied to any supersaturation profile as a function of antisolvent composition (instead of addition rate).

Application of this approach to a nominal model for the seeded antisolvent batch crystallization of paracetamol in an acetone−water mixture[29,30] results in very good tracking of the supersaturation setpoint profile (Figure 3), producing uniform growth of the seed crystals with negligible nucleation. The following sections analyze the sensitivity and robustness of the concentration control approach in antisolvent crystallization with comparison to the control system where the supersaturation setpoint is specified as an explicit function of time. These results complement earlier studies that were performed for cooling crystallization.[2,28]

3. Supersaturation Profiles for Antisolvent Crystallization

In this section, the application of different supersaturation profiles for seeded antisolvent crystallization is discussed. The analysis focuses on nucleation and growth, neglecting agglomeration and breakage. The antisolvent crystallization kinetic expressions were inspired by Granberg et al.[29] The nucleation rate is

$$B\ (\text{no. of particles/m}^3\ \text{s}) = k_b\Delta c^b \tag{6}$$

$$k_b = 4.338 \times 10^{58} \exp(-1.374w) \quad (60\% \le w \le 80\%) \tag{7}$$

$$b = 1.997 \times 10^{-3}w^2 - 6.237 \times 10^{-1}w + 4.042 \times 10^{1} \quad (60\% \le w \le 80\%) \tag{8}$$

and the growth rate is

$$G\ (\text{m/s}) = k_g\Delta c^g \tag{9}$$

$$k_g = -9.6300 \times 10^{-11}w^3 + 3.3558 \times 10^{-8}w^2 - 1.2606 \times 10^{-6}w + 3.6852 \times 10^{-5} \tag{10}$$

$$g = -1.108 \times 10^{-4}w^2 + 1.024 \times 10^{-2}w + 1.427 \tag{11}$$

where Δc (kg solute/kg solvents) $= c - c^*$ and w is the mass percent of antisolvent on a solute-free basis. The solubility curve at 16 °C is given by[30]

$$c^* = 1.302 \times 10^{-6}w^3 - 1.882 \times 10^{-4}w^2 - 2.237 \times 10^{-4}w - 5.746 \times 10^{-1} \ (60\% \le w \le 80\%) \tag{12}$$

Secondary nucleation is neglected due to the low solids density of this particular system.

As both nucleation and growth rates increase with antisolvent composition, operating a seeded crystallizer at constant supersaturation can result in nucleation occurring toward the end of the batch as the antisolvent composition increases. Such dependence is also expected for secondary nucleation when solids density is significant. Thus, a supersaturation profile that maximizes growth and minimizes nucleation for the operating range of antisolvent composition must be determined. By setting a constant tradeoff between growth and nucleation rates, a supersaturation profile can be computed by

$$K = \frac{G}{B} = \frac{k_g\Delta c^g}{k_b\Delta c^b} \Rightarrow \Delta c = \left(K\frac{k_b}{k_g}\right)^{1/(g-b)} \tag{13}$$

where K is a tradeoff ratio between growth and nucleation rates constrained by achieving a targeted yield within a specified batch time. If the kinetic constants are weak functions of antisolvent composition, a constant supersaturation profile would suffice.[31,32]

The number- and weight-mean size and yield for antisolvent addition rates based on different constant supersaturations, constant tradeoff, and constant relative supersaturation are reported in Table 1. The values were computed by the method of moments and mass balances (see ref 33 for definitions of moments and the model equations), assuming a well-mixed crystallizer, using Matlab 7.0.1. Figure 4 shows the supersaturation profile as a function of antisolvent composition for the case of constant tradeoff and constant relative supersaturation.

Table 1. Comparison between Four Supersaturation Profiles[a]

case	number-mean size (μm)	weight-mean size (μm)	yield (%)
initial condition			
saturated solution with 60% antisolvent, seed mass = 0.4125 g	187.50	195.65	0.00
case A			
"low" constant supersaturation, $\Delta c = 0.01$ kg/kg	450.76	478.65	36.36
case B			
"high" constant supersaturation, $\Delta c = 0.01105$ kg/kg	465.35	553.11	53.54
case C			
constant tradeoff, $K = 7 \times 10^{-6}$ (mm/s)/(no. of particles/m^3 s)	484.94	556.38	53.02
case D			
constant relative supersaturation, $\Delta c/c^* = 0.09$	484.01	556.76	53.73

[a] The simulation is for a batch time of 2 h, initial volume of 300 mL, maximum volume of 500 mL, and maximum flow rate of antisolvent of 6 mL/min.

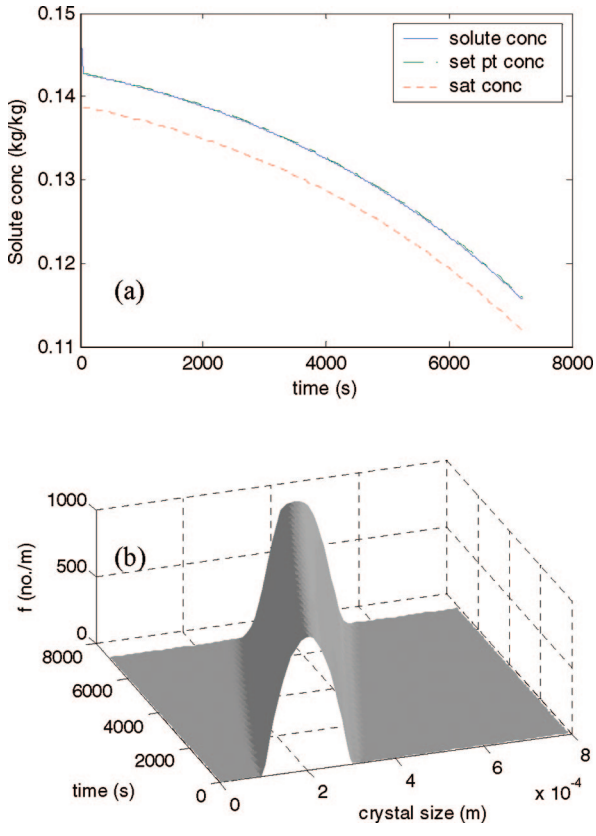

Figure 3. (a) The supersaturation and concentration profiles and (b) product crystal size distribution during the simulated seeded antisolvent crystallization of paracetamol in acetone−water mixture with concentration control. The simulation uses a sampling time $t_s = 60$ s, a constant supersaturation setpoint $\Delta c = 0.004$ kg solute/kg solvents, and a seed amount of 1.586 g/kg solvents over a batch time of 2 h.

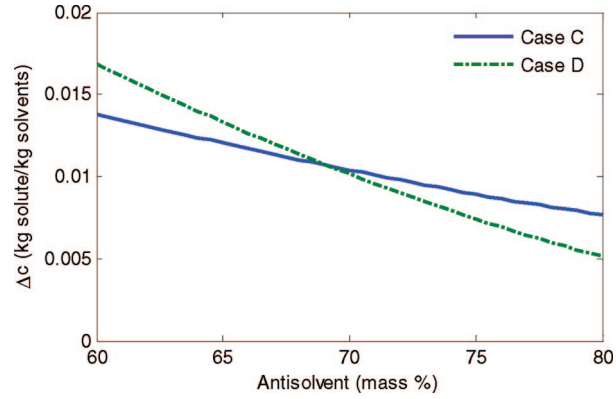

Figure 4. Supersaturation profiles based on constant relative supersaturation and constant tradeoff listed in Table 1.

While a low constant supersaturation profile (case A in Table 1) results in negligible nucleation, the yield is significantly lower and a longer batch time would be required to achieve a higher yield. On increasing the constant supersaturation (case B in Table 1), the crystals grow much larger (greater weight-mean size) and a higher yield is obtained, but there is more nucleation toward the end of the batch (see the μ_0 plot in Figure 5), which can cause problems in the subsequent filtration and drying processes.

The values of the constant supersaturation and constant relative supersaturation (cases B and D, respectively) in Table 1 were chosen to give approximately the same yield as the constant tradeoff case (case C), so the three cases can be compared on a consistent basis. The supersaturation profile based on constant tradeoff (case C) decreases with increasing antisolvent composition for this system, which gives a qualitatively different antisolvent addition rate profile compared to constant supersaturation (see Figure 6). Maintaining a constant tradeoff (case C) results in a steady increase in nucleated crystals, but following a constant supersaturation (case B) produces more nucleation near the end of the batch (Figure 5). Case B produced more fine crystals (smaller number-mean size in Table 1), as the crystals nucleated near the end of the batch have less time to grow. The supersaturation profile obtained based on constant relative supersaturation (case D) is qualitatively similar to that of a constant tradeoff (case C), but more pronounced, which results in increased nucleation (see the μ_0 plot in Figure 5). Crystal product quality in terms of number and weight-mean size and yield is similar for both cases. This suggests that, for this system, if the kinetic parameters were not available, then several constant relative supersaturation profiles could be evaluated experimentally to converge to nearly the same operations as case C (which required kinetic parameters to compute). Alternatively, an automated approach[24] could be used for the systematic experimental convergence of the supersaturation profile toward the optimal setpoint profile.

4. Comparison between Direct Operation and Concentration Control: Simulation Results

The antisolvent addition rate profile as a function of time obtained from case C can be directly implemented to a batch crystallizer as a function of time (referred to as *direct operation*, which is the dominant implementation in industrial practice), or the antisolvent addition rate can be computed according to the desired supersaturation profile based on measured concentrations of solute and solvents at each sampling instance (concentration control). Direct operation is analogous to the T-control strategy for cooling crystallization.[2] *Concentration control* implements feedback based on a concentration measurement

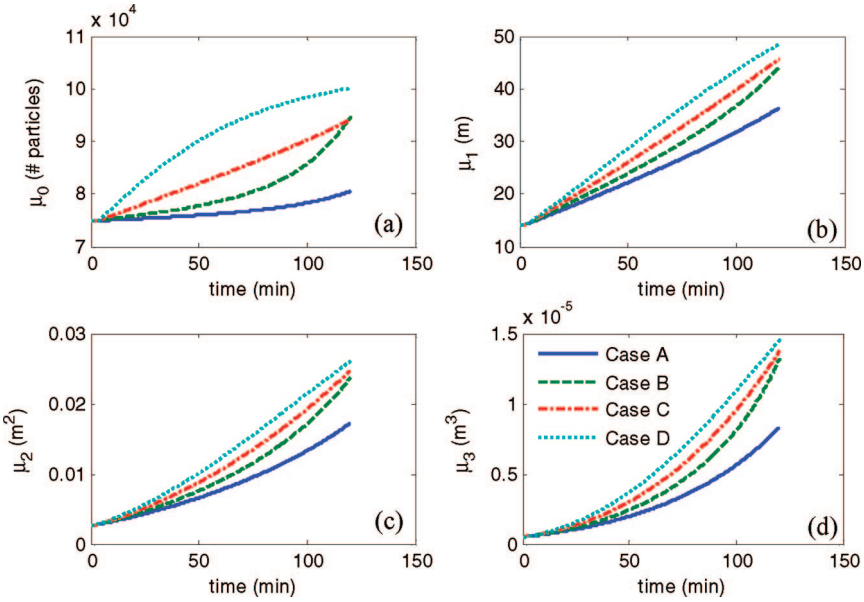

Figure 5. (a) Zeroth-, (b) first-, (c) second-, and (d) fourth-order moments obtained from supersaturation profiles listed in Table 1.

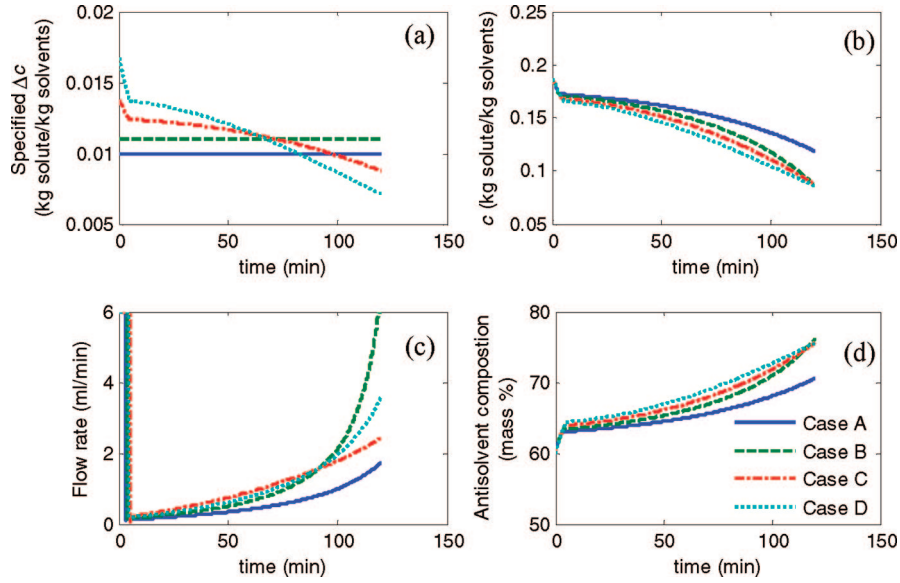

Figure 6. Variation of (a) supersaturation Δc, (b) concentration c, (c) antisolvent flow rate, and (d) antisolvent composition with time from supersaturation profiles listed in Table 1.

without any prior knowledge of the crystallization kinetics, to experimentally converge to a supersaturation profile that falls between the solubility curve and the metastable limit of the system. The goal of this section is to compare the direct operation and concentration control approaches for operating an antisolvent crystallizer, to assess the relative merits of each.

For specificity, the supersaturation profile for case C was used in the comparison. While the direct operation approach has a fixed batch time of 2 h, the concentration control approach was set to meet a yield of 53% with a flexible batch time (maximum batch time set at 10 h). The concentration measurements are assumed to be made every 30 s, which is a sufficient sampling time for ATR-FTIR spectroscopy. Figure 7 shows the time profile for the antisolvent flow rate, antisolvent composition, supersaturation, and solute concentration. There is an initial sharp increase in antisolvent composition to create the supersaturation from the initial saturated solution. This is followed by a slow reduction in the supersaturation setpoint according to the supersaturation profile shown in Figure 4. Figure 7 also indicates that the concentration control approach follows the supersaturation setpoint closely. There is slight drift toward the end of the batch due to an increase in growth and nucleation rates at higher antisolvent composition and an increase in desupersaturation rate as a consequence of the increase in crystal surface area. This drift can be reduced to a negligible value by selecting a shorter sampling time (the sampling time can be reduced to 1 s using a modern FTIR spectrometer using 1 scan per measurement).

Table 2 reports the sensitivities of both operating strategies to disturbances. For the disturbances in the antisolvent flow rate, the initial mass of antisolvent, and the nucleation prefactor k_b, small deviations in the crystal product quality and yield are observed for direct operation. Concentration control is less sensitive to the former two disturbances, especially for achieving the target yield. The yield for direct operation is very sensitive to the evaporation of some of the

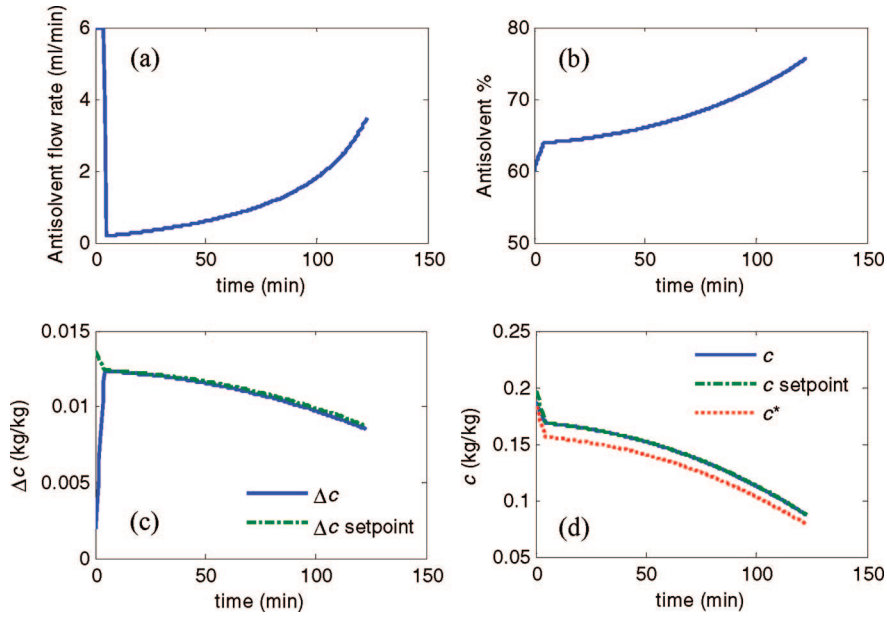

Figure 7. (a) Antisolvent flow rate, (b) antisolvent %, (c) supersaturation, and (d) solute concentration as a function time by the concentration control approach following the supersaturation profile for case C shown in Figure 1. Sampling time = 30 s. Maximum flow rate = 6 mL/min.

Table 2. Computed Sensitivities of Direct Operation and Concentration Control to Disturbances According to Supersaturation Profile in Case C[a]

		relative error (%)						
		number-mean size		weight-mean size		yield		batch time for C-control (h)
disturbance		direct operation	C-control	direct operation	C-control	direct operation	C-control	
shift in solubility curve	−5%	−17.15	−42.218	−12.63	−23.7589	5.88	0.55	0.9
	+5%	−15.69	15.0594	−6.86	2.0294	−5.57	−0.1333	8.1083
error in antisolvent flow rate	−5%	−0.61	0.1564	−1.00	0.1335	−2.97	0.2773	2.05
	+5%	0.38	0.0597	0.79	0.1234	2.80	0.3278	2.0417
variation in initial mass of antisolvent	+5%	−0.68	0.2939	−1.05	0.1025	3.09	0.1435	2.025
variation in initial mass of solvent	−5%	−35.56	5.2884	−30.11	4.9384	8.55	0.1106	2.15
evaporation of solvent (organic)	4 g/h	−2.72	7.0586	4.75	7.683	10.00	−0.1708	2.225
	6 g/h	−7.40	4.6532	3.12	8.1689	14.85	0.1387	2.15
error in k_g	−20%	−16.59	−3.2831	−4.02	−0.5837	−1.50	0.0249	2.525
	−10%	−7.10	−1.4649	−1.67	−0.2163	−0.68	0.1213	2.2583
	+10%	5.16	1.3209	1.24	0.2626	0.57	0.0916	1.8667
	+20%	8.88	2.3381	2.20	0.3404	1.05	−0.17	1.7167
error in g	−20%	24.68	15.8285	9.43	4.367	6.15	0.3576	0.5833
	−10%	20.29	8.1858	6.39	1.3745	3.69	−0.2003	1.0333
	+10%	−52.71	−12.1326	−19.33	−2.3829	−5.10	−0.017	4.0917
	+20%	−74.27	−27.0125	−47.54	−6.586	−10.56	−0.1873	8.2083
error in k_b	−20%	2.69	2.5645	0.44	0.3267	−0.02	−0.2304	2.0417
	−10%	1.31	1.257	0.22	0.1628	−0.01	−0.1152	2.0417
	+10%	−1.26	−1.2093	−0.22	−0.1618	0.01	0.1151	2.0417
	+20%	−2.46	−2.3736	−0.43	−0.3225	0.02	0.2302	2.0417
error in b	−20%	−74.37	−79.0073	−73.20	−75.0598	5.25	0.1636	0.9167
	−10%	−46.56	−53.0406	−31.70	−32.818	2.09	−0.2322	1.7083
	+10%	15.58	14.9769	2.21	2.1859	−0.12	0.097	2.0583
	+20%	16.54	15.8636	2.25	2.235	−0.18	0.0677	2.0583
Include Crystal Count Measurement for Direct Design								
shift in solubility curve	−5%	−17.15	−3.6881	−12.63	−2.577	5.88	−0.0139	1.9458
error in b	−20%	−74.37	−46.3718	−73.20	−29.4008	5.25	−0.0283	7.0639
	−10%	−46.56	−11.1888	−31.70	−10.4301	2.09	−0.0431	6.6056

[a] Direct operation: batch time = 2 h. Concentration control: target yield = 53%, maximum batch time = 10 h, concentration sampling time = 30 s. Concentration control with crystal count: crystal count sampling time = 5 s; once the crystal count is detected to be greater than 7.7×10^4 in less than 12 min, the supersaturation setpoint is set to 40% of the original supersaturation profile and the antisolvent flow rate is set to zero.

organic solvent, where concentration control produces larger crystals with small change in the yield. Concentration control is much less sensitive than direct operation to variations in the growth kinetics (k_g and g).

For a positive shift in the solubility curve or in the nucleation exponent b, which both result in a decrease in nucleation, concentration control results in larger crystals for the targeted yield. However, when there is a negative shift in the solubility curve or in the nucleation exponent b, both direct operation and concentration control result in large deviations in mean crystal size due to excessive nucleation at the early stage of the batch while following the supersaturation setpoint (see Figure 8). The lower sensitivity of concentration control to all of the disturbances except for these two motivates the development of a

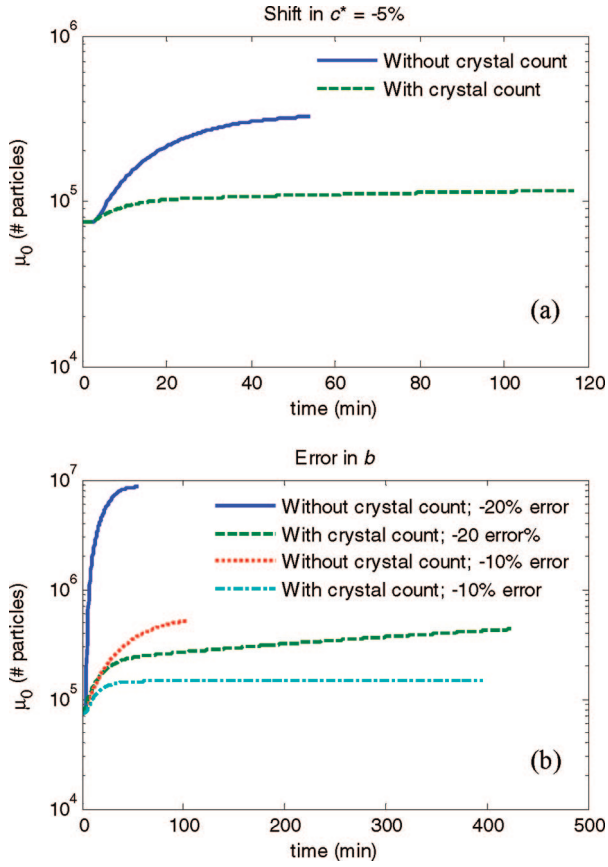

Figure 8. Variation of the number of particles with time using the concentration control approach, both with and without using crystal count measurement, for disturbances that affect nucleation: (a) 5% shift in c^* and (b) error in b. Laser backscattering sampling time = 5 s.

modification of the concentration control approach specifically designed to handle disturbances that create unexpected large nucleation.

Most of the problems in crystallization operation are due to uncontrolled nucleation events. The majority of batch recipes have the objective to identify operating conditions that suppress undesired nucleation. The sensitivity of the concentration control approach to disturbances that result in uncontrolled nucleation can be reduced by including crystal count measurement to detect the onset of excessive nucleation, commonly used in the detection of the metastable limit[19,24] as well as in some feedback control schemes.[25,34,35] The most commonly used sensor for estimating the number of crystals is laser backscattering, for which the most commonly used sensor used in industry is the Lasentec focused beam reflectance measurement (FBRM) probe. While crystals much smaller than ~1 μm cannot be measured by laser backscattering, the high supersaturation that nucleates such crystals causes the nuclei to grow rapidly to detectable size. An increase in the total number of crystals counted per second, commonly referred to as the "total counts/s" or "counts/s," indicates that excessive nucleation has been detected.[19] The paper proposes two approaches that can be used to incorporate the in situ laser backscattering measurement to adapt the concentration control to changing process conditions. In the first approach, once excessive nucleation is detected, the supersaturation setpoint is reduced and antisolvent addition halted until the new supersaturation setpoint is reached. (Sudden stopping of the antisolvent addition flow can be done at the bench scale by using a peristaltic or syringe pump. At the manufacturing scale, the flow can be stopped suddenly by using a three-way valve that shifts the antisolvent addition flow to recycle.) The crystal counts/s can be measured at a rate of every 5 s for the most common commercial laser backscattering sensor (FBRM). In the simulations, *excessive* nucleation was detected when the increase in the counts/s was greater than 10% of the expected increase in nuclei (with no disturbances) within the first 12 min. Subsequently, the supersaturation profile was reduced to 40%, in magnitude, of the original supersaturation profile.

Figure 8 and the last two rows in Table 2 show the simulation results with this approach. The inclusion of the measurement of counts/s provided a significant reduction in the sensitivity of the concentration control approach to disturbances that cause unexpected nucleation events. Nevertheless, the improvement would vary with different systems and with the extent to which the supersaturation is reduced. Thus, for solute−solvents systems in which the nucleation kinetics or solubility vary widely due to variations in the contaminant profiles in the chemical feedstocks, the solubility curve and the metastable limit can be measured for every new batch to determine the desired supersaturation profile. Such measurements can be done with little effort with software that fully automates the experimental procedure.[24] The next section presents a feedback control approach of using in situ laser backscattering, which utilizes a cascade proportional-integral control algorithm that adapts the supersaturation profile in correlation with the extent of the nucleation and corrects the desired counts/s by generating fines dissolution by driving the process below the solubility curve.

5. Experimental Implementation of Adaptive Concentration Control using in Situ Laser Backscattering

5.1. Materials and Equipment. The experiments were performed using pharmaceutical-grade paracetamol (4-aminodiphenol, 98% purity, obtained from Aldrich) in a 500-mL jacketed round-bottom flask with an overhead stirrer. 2-Propanol of laboratory grade was used in all tests. The temperature was measured using a Fluke 80TK Teflon-coated thermocouple module connected to a computer, and it was controlled by ratioing hot and cold water using a research control valve (Badger Meter, Inc.) via a proportional-integral computer control system designed via internal model control. The total particle counts per second and chord length distributions of the paracetamol crystals in solution were measured using a Lasentec FBRM in situ laser backscattering probe connected to a Pentium III running version 6.0b9 of the FBRM Control Interface software. The IR spectra of the paracetamol solution were measured using a DIPPER-210 ATR immersion probe with two reflections (Axiom Analytical) with ZnSe as the internal reflectance element. The probe was attached to a Nicolet Protégé 460 FTIR spectrophotometer connected to a Pentium II computer running OMNIC 4.1a software from Nicolet Instrument Corp. The spectrophotometer was purged with nitrogen gas 1 h before and while measurements were taken to reduce the effect of CO_2 absorption in its optical path. Temperature readings were collected every 2 s and averaged during the collection of each spectra, which consisted of 32 scans (at 1 min intervals). The two computers connected to the instruments were supervised by a fourth master computer via software written in Labview (National Instruments), which implemented the nucleation control algorithm. The experimental setup is shown schematically in Figure 9.

6. Evaluation of Adaptive Concentration Control

The control architecture implemented on the supervisory computer is shown in Figure 10. The control structure is exemplified for an antisolvent system, but the method is the same and works similarly for cooling crystallization. In addition to the concentration controller, another proportional-integral (PI) controller was used to adapt the supersaturation profile $\Delta c_{set}(w)$ [or $\Delta c_{set}(T)$ for cooling systems]. The total counts/s from in situ laser backscattering was compared to

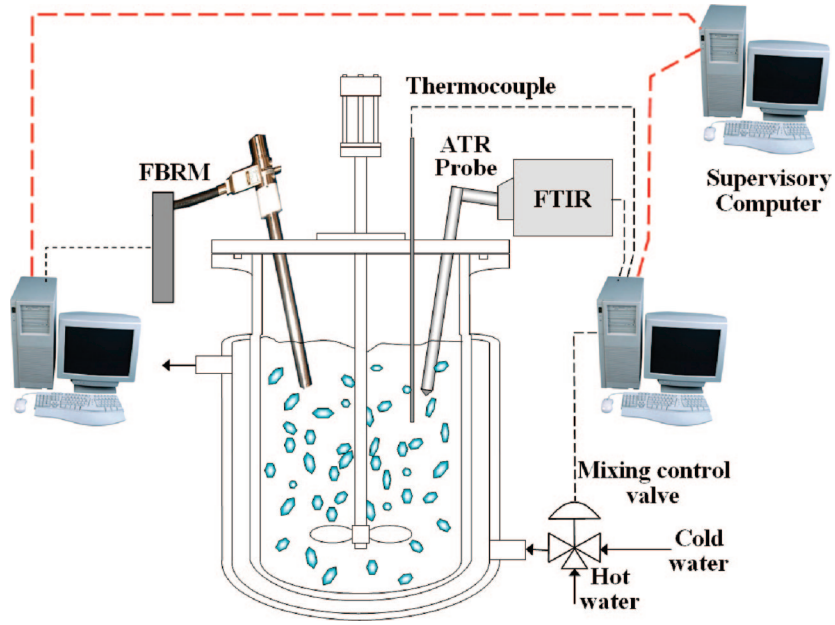

Figure 9. Schematic representation of the experimental setup with the supervisory computer used to implement the adaptive concentration control strategy.

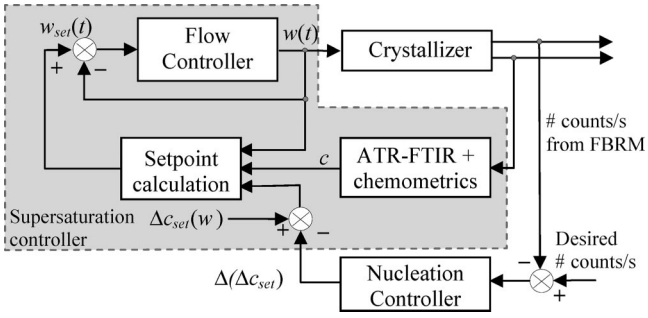

Figure 10. Schematic diagram of the adaptive concentration control system using FBRM measurements.

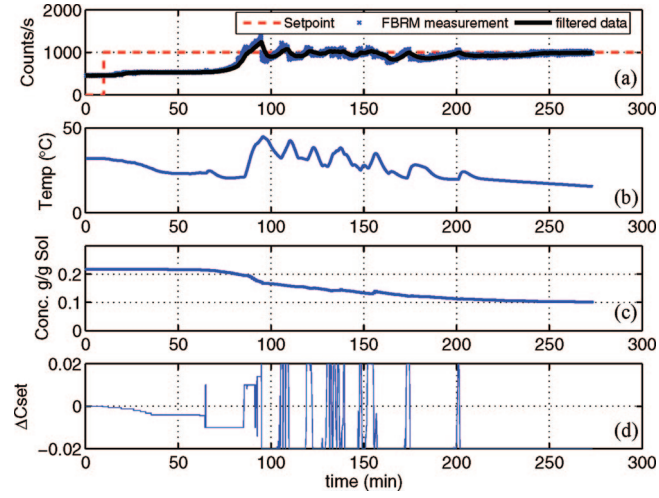

Figure 11. Experimental results for the cascade adaptive concentration control of the batch cooling crystallization of paracetamol in 2-propanol: (a) FBRM counts/s (raw measurement and filtered signal) with the setpoint value, (b) temperature measurement, (c) solute concentration, and (d) control output from nucleation controller as changes to the supersaturation setpoint values. The total time of temperature increase is less than 1 h during the duration of the experiment, and the concentration is decreasing for the vast majority of the experiment.

the desired value and the supersaturation profile increased or decreased by a $\Delta(\Delta c_{set})$ amount calculated according to the higher level PI controller. The desired value for the counts/s can be determined from previous experiments in the case of an unseeded crystallization, and for a seeded crystallization it can be set to the value indicated by laser backscattering after the introduction of the seed. The experimental results with the adaptive concentration control for the more challenging case of an unseeded cooling crystallization of paracetamol in 2-propanol are shown in Figure 11. The supersaturation profile was adapted by the master controller based on filtered FBRM measurements. Filtering the FBRM data eliminated any excessive reaction of the concentration control system to fluctuations in the total number of counts due to noise rather than nucleation or dissolution. The desired number of counts per second was set to 1000 in the experiments. The adaptive control decreased the temperature until primary nucleation occurred, after which the profile was adapted to maintain the desired counts/s. The resulted temperature profile shows oscillations, as short bursts of increased temperature dissolved excess crystals. Once the counts/s exceeds the desired value, the controller automatically drives the process below the solubility curve to dissolve the fine (small) crystals, correcting the counts/s. When the counts/s was within desired limits of the setpoint (±5% in the reported experiments), the master controller was not active. When the counts/s was below the desired value, the supersaturation was increased until nucleation was detected and the counts/s corrected. The change in the supersaturation was constrained to ±0.02, controlled by using a PI controller with antiwindup compensation. The adaptive feature of the proposed controller can be understood better by looking at the operating curve in the phase diagram (Figure 12, which is exactly the same as the state-space trajectory for this system). Although the operating curve was coarse, since concentration measurements were only available at 1-min intervals, within which the temperature could change significantly, Figure 12 illustrates very well the main features of the control approach. The cooling crystallization of

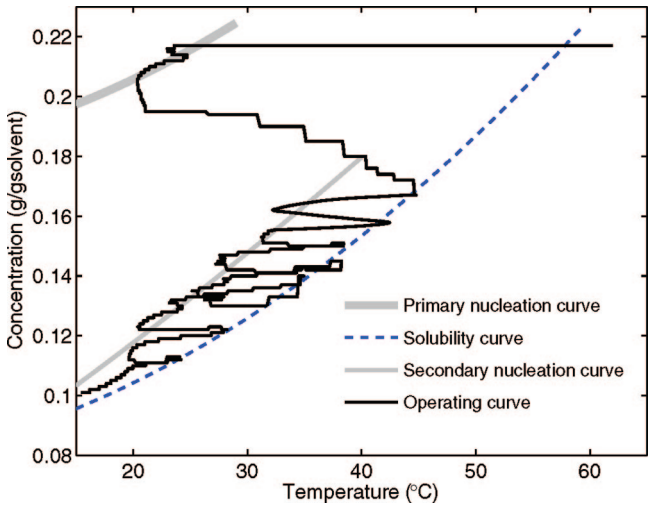

Figure 12. Experimental operating curve with detected primary and secondary nucleation curves in the phase diagram for the unseeded cooling crystallization of paracetamol in 2-propanol as obtained with adaptive concentration control.

paracetamol in 2-propanol is characterized by a very broad primary metastable zone width typical of organic crystals. The temperature initially had to be decreased significantly to generate primary nucleation. Primary nucleation at such high superstaturation is very fast, making the control of nucleation very difficult. FBRM measurements were available at every 5 s, but the noise in the total counts can be large enough in a particular application that either a larger sample interval or a filter should be used, which would delay the detection of the fast nucleation event. Additionally, submicron nuclei that form are not detected by the FBRM until enough such crystals grow to detectable size. These considerations will inevitably lead to an overshoot in the counts/s compared to the desired value of 1000. Then the controller drove the process into the dissolution zone by increasing the temperature. Since newly formed crystals at this stage are very small and dissolution kinetics tend to be very fast, a short time period below the solubility curve can reduce the counts/s. Since the dissolution rate is a strong function of the size of the crystals, the extent to which the operating curve will cross the equilibrium curve depends on the size of the crystals. The antiwindup feature of the control algorithm allowed fast switching from heating to cooling to avoid excessive undershoot caused by the inertia of the system, which could generate complete dissolution of the crystals. Due to the presence of crystals in the system (generated via primary nucleation), secondary nucleation becomes dominant, which results in a significantly narrower metastable zone width (Figure 12). The adaptive control algorithm demonstrated an excellent ability to detect the new metastable zone width during the crystallization process. The metastable zone width becomes narrower as the amount of solids in the slurry increases, which is consistent with crystallization theory. The cascade structure resulted in very robust crystallization control, while automatically detecting both the metastable and solubility curves and adapting the operating curve accordingly during operation. The only information needed a priori is a specification for the setpoint on the total counts/s for the unseeded crystallization, or an appropriate seeding point for a seeded system. This approach is very robust against errors in the concentration measurement, which is the major weakness of the alternative

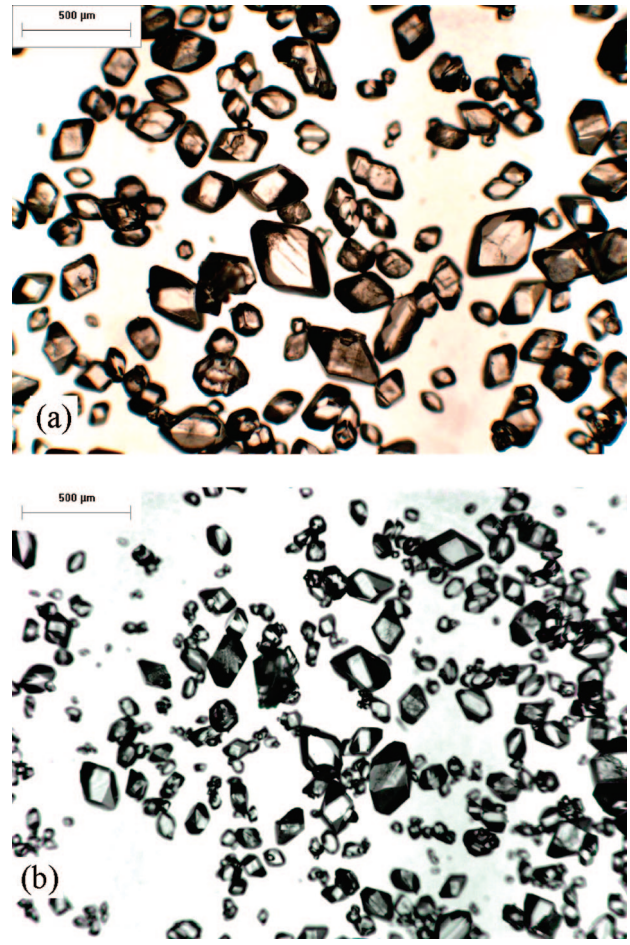

Figure 13. Microscopic images of the paracetamol crystals obtained from 2-propanol by using (a) adaptive concentration control and (b) linear cooling.

approaches that use only concentration measurement in the feedback control of crystallization. This adaptive control algorithm is completely insensitive to drift in the concentration measurement, which likely occurred since the experiment in Figure 11 was for ~5 h. The cascade control architecture adapted the supersaturation profile to maintain the desired total counts/s, despite any drift or bias in the concentration measurement. The tuning of the control system must be done with some care, due to the very different dynamics of the system in different operating zones (e.g., during nucleation or dissolution). Although the resulting "oscillating" operating curve seems unconventional at first sight, it provides an adaptive operation that is very robust against scale-up, changes in seed quality, presence of impurities, etc. Operation of a batch crystallization according to the adaptive procedure resembles the fines removal approach well-known in crystallization practice, in which the fines are removed through a properly designed fine segregation device. The adaptive approach provides a *fines removal* technique via operation with no additional equipment or design needed. Figure 13 shows the microscopic images of the product obtained with adaptive concentration control and using constant cooling rate at 0.075 °C/min with no adaptation of the operating curve. The adaptive approach yielded superior crystal quality with larger average crystal size. This observation was also supported by the FBRM chord length distribution measurements at the end of the batch, shown in Figure 14.

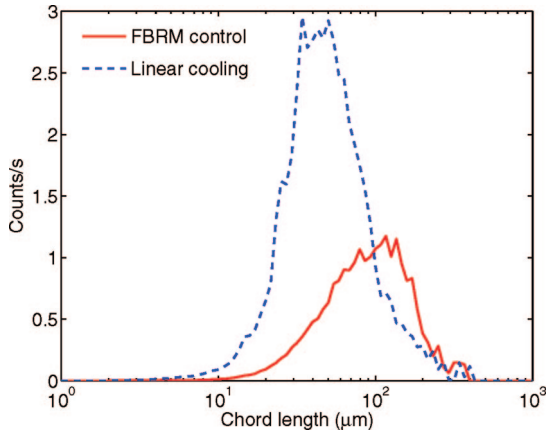

Figure 14. Square-weighted CLD of the products obtained using linear cooling and adaptive concentration control (labeled as "FBRM control"). The CLD for linear cooling is broader and has a smaller mean.

These experiments implemented the unseeded case, as this is more challenging than operations with seeding in the metastable zone. In addition to the standard advantages of increasing crystal purity and reducing potential for solvent inclusions, seeded operations would lead to a much smaller initial increase in the temperature than shown in Figure 11b, which would reduce batch time and increase productivity. Further, the setpoint for the nucleation controller is much easier to specify for seeded operations, as it can be based on the FBRM measurement shortly after seeding.

7. Conclusions

The analysis presented in the paper shows that the combination of concentration (supersaturation) control with total count measurement can provide low sensitivity to process disturbances and variations in solubility and nucleation and growth kinetics, whereas the direct specification of the antisolvent addition rate or temperature profile in batch recipe is inherently sensitive to many disturbances. The batch time is not fixed for concentration control, since the rate at which the process moves along the setpoint trajectory is determined by the crystallization kinetics. Although this might result in a change in how the manufacturing process is scheduled, variability in the production time is certainly preferable over variability in product quality in pharmaceutical production. Since it has been shown that an optimal or nearly optimal supersaturation setpoint trajectory can be determined with an automated experimental system,[24] the tracking of such a setpoint using the concentration control strategy eliminates the need to develop highly accurate first-principles models by in situ measurement of the concentrations and particle size distributions. Hence, the proposed approach can significantly reduce the time required for developing new antisolvent or cooling crystallization processes. Additionally, adaptive concentration control utilizing in situ laser backscattering provides a very robust engineering approach for crystallization control that required minimal a priori information. While such an approach may produce increased variation in temperature or other variables, it can lead to reduced variation to the product quality variables of importance.

Although many of the observations in this paper were obtained for particular crystallization systems, these observations are expected to hold for other crystal-solvent systems given the inherent ability of concentration control to correct for most disturbances and the inherent inability of direct operation to suppress the effects of most disturbances. For an antisolvent crystallization, the total counts/s signal to the adaptive controller would be revised to include the effect of dilution on the FBRM, and the addition of solvent to create short bursts of undersaturation to dissolve fine crystals would be limited to keep the solution volume and liquid−liquid separations costs low. While an experienced control or crystallization expert could have postulated the observations in the paper by using intuition, the analysis of a specific system provides some estimates of the relative magnitude of the effects of disturbances on the two approaches to operating antisolvent or cooling crystallizers and confirms the relative effectiveness of the use of total count measurement to reducing the sensitivity to disturbances that induce unexpected excessive nucleation. Given that concentration control has already been implemented on antisolvent and cooling crystallizers in industry,[24] the results indicate that the small additional step of including total count measurement would lead to especially robust industrial implementations of crystallizer control.

Acknowledgment. X.Y.W. acknowledges the Singapore Agency for Sciences, Technology, and Research for her research scholarship, and Z.K.N. acknowledges financial support from the Engineering and Physical Sciences Research Council (EPSRC), U.K. (EP/E022294/1).

References

(1) Braatz, R. D. *Annu. Rev. Control* **2002**, *26*, 87–99.
(2) Fujiwara, M.; Nagy, Z. K.; Chew, J. W.; Braatz, R. D. *J. Process Control* **2005**, *15*, 493–504.
(3) Larsen, P. A.; Patience, D. B.; Rawlings, J. B. *IEEE Control Syst. Mag.* **2006**, *26*, 70–80.
(4) Paul, E. L.; Tung, H. H.; Midler, M. *Powder Technol.* **2005**, *150*, 133–143.
(5) Braatz, R. D.; Fujiwara, M.; Ma, D. L.; Togkalidou, T.; Tafti, D. K. *Int. J. Mod. Phys. B* **2002**, *16*, 346–353.
(6) Yu, L. X.; Lionberger, R. A.; Raw, A. S.; D'Costa, R.; Wu, H. Q.; Hussain, A. S. *Adv. Drug Delivery Rev.* **2004**, *56*, 349–369.
(7) Barrett, P.; Smith, B.; Worlitschek, J.; Bracken, V.; O'Sullivan, B.; O'Grady, D. *Org. Process Res. Dev.* **2005**, *9*, 348–355.
(8) Birch, M.; Fussell, S. J.; Higginson, P. D.; McDowall, N.; Marziano, I. *Org. Process Res. Dev.* **2005**, *9*, 360–364.
(9) Chung, S. H.; Ma, D. L.; Braatz, R. D. *Can. J. Chem. Eng.* **1999**, *77*, 590–596.
(10) Ma, D. L.; Tafti, D. K.; Braatz, R. D. *Comput. Chem. Eng.* **2002**, *26*, 1103–1116.
(11) Sarkar, D.; Rohani, S.; Jutan, A. *Chem. Eng. Sci.* **2006**, *61*, 5282–5295.
(12) Togkalidou, T.; Tung, H. H.; Sun, Y.; Andrews, A. T.; Braatz, R. D. *Ind. Eng. Chem. Res.* **2004**, *43*, 6168–6181.
(13) Ward, J. D.; Mellichamp, D. A.; Doherty, M. F. *AIChE J.* **2006**, *52*, 2046–2054.
(14) Worlitschek, J.; Mazzotti, M. *Cryst. Growth Des.* **2004**, *4*, 891–903.
(15) Chung, S. H.; Ma, D. L.; Braatz, R. D. *Chemom. Intell. Lab. Syst.* **2000**, *50*, 83–90.
(16) Gunawan, R.; Ma, D. L.; Fujiwara, M.; Braatz, R. D. *Int. J. Mod. Phys. B* **2002**, *16*, 367–374.
(17) Ma, D. L.; Braatz, R. D. *Comput. Chem. Eng.* **2003**, *27*, 1175–1184.
(18) Ma, D. L.; Chung, S. H.; Braatz, R. D. *AIChE J.* **1999**, *45*, 1469–1476.
(19) Fujiwara, M.; Chow, P. S.; Ma, D. L.; Braatz, R. D. *Cryst. Growth Des.* **2002**, *2*, 363–370.
(20) Gron, H.; Borissova, A.; Roberts, K. J. *Ind. Eng. Chem. Res.* **2003**, *42*, 198–206.
(21) Yu, Z. Q.; Chow, P. S.; Tan, R. B. H. *Ind. Eng. Chem. Res.* **2006**, *45*, 438–444.
(22) Liotta, V.; Sabesan, V. *Org. Process Res. Dev.* **2004**, *8*, 488–494.

(23) Nonoyama, N.; Hanaki, K.; Yabuki, Y. *Org. Process Res. Dev.* **2006**, *10*, 727–732.
(24) Zhou, G. X.; Fujiwara, M.; Woo, X. Y.; Rusli, E.; Tung, H. H.; Starbuck, C.; Davidson, O.; Ge, Z. H.; Braatz, R. D. *Cryst. Growth Des.* **2006**, *6*, 892–898.
(25) Doki, N.; Seki, H.; Takano, K.; Asatani, H.; Yokota, M.; Kubota, N. *Cryst. Growth Des.* **2004**, *4*, 949–953.
(26) Sheikhzadeh, M.; Trifkovic, M.; Rohani, R. *Chem. Eng. Sci.* **2008**, *63*, 991–1002.
(27) Sheikhzadeh, M.; Trifkovic, M.; Rohani, R. *Chem. Eng. Sci.* **2008**, *63*, 1261–1272.
(28) Nagy, Z. K.; Chew, J. W.; Fujiwara, M.; Braatz, R. D. In *Advanced Control of Chemical Processes (ADCHEM)*; Allgower, F., Gao, F., Eds.; Elsevier: Amsterdam, The Netherlands, 2004; pp 83−90.
(29) Granberg, R. A.; Bloch, D. G.; Rasmuson, A. C. *J. Cryst. Growth* **1999**, *199*, 1287–1293.
(30) Granberg, R. A.; Rasmuson, A. C. *J. Chem. Eng. Data* **2000**, *45*, 478–483.
(31) Jones, A. G.; Mullin, J. W. *Chem. Eng. Sci.* **1974**, *29*, 105–118.
(32) Mullin, J. W.; Nyvlt, J. *Chem. Eng. Sci.* **1971**, *26*, 369–377.
(33) Randolph, A. D.; Larson, M. A. *Theory of Particulate Processes*, 2nd ed.; Academic Press: New York, 1988.
(34) Chew, J. W.; Chow, P. S.; Tan, R. B. H. *Cryst. Growth Des.* **2007**, *7*, 1416–1422.
(35) Tadayyon, A.; Rohani, S. *Can. J. Chem. Eng.* **2000**, *78*, 663–673.

CG800131R